Dandao Xuebao/Journal of Ballistics
ISSN: 1004-499X
Vol. 36 No. 1 (2024)

Significant Improvement in Mild Steel Mechanical Properties with Cu-Fe-Ti Alloy Coatings

Muhammad Zahid Khan*[1], Muhammad Rehan[2], Faisal Mehmood[3], Muhammad Yousaf Talpur[3], Munsif Ali[4], Muhammad Tariq[4]

1. Department of Physics Gomal University Dera Ismail Khan, 29111, KPK, Pakistan

2. Department of Physics, The University of Lahore, Sub-campus Sargodha, 40100, Pakistan

3. Bioenergy and Environment Science & Technology Laboratory, College of Engineering, China Agricultural University, Beijing 100107, PR China

4. Department of Physics, University of Peshawar, 25000, Pakistan

*__Corresponding Author__: Muhammad Zahid Khan

*****Department of Physics Gomal University Dera Ismail Khan, 29111, KPK, Pakistan

*__Email:__ muhammadzahidk961@gmail.com

Abstract

This research examines the mechanical properties of mild steel using the electrodeposition of ternary Cu-Fe-Ti alloys with varying Ti compositions at room temperature. The coating process maintained constant pH, current density, deposition time, and temperature. X-ray diffraction analysis revealed single-phase compositions with a face-centered cubic (fcc) structure for all electrodeposited samples. The crystallite sizes ranged from 14-17 nm. The lattice parameters of the Cu-Fe-Ti alloys strongly depended on the Ti concentration. Scanning electron microscopy images showed smoother surfaces with increasing Ti content. Energy-dispersive X-ray spectroscopy confirmed the presence of Cu, Fe, and Ti in the coatings. The Vicker hardness increased from 255 HV to 444 HV. With more Ti in solution, the Cu-Fe-Ti alloy coating thickness on mild steel decreased from 63 μm to 25 μm, and the surfaces became smoother. Thus, the improved mechanical properties correlate with Ti concentration, lattice parameter, crystallite size, and coating thickness. Enhanced mechanical properties of mild steel with Cu-Fe-Ti alloy coatings offer potential for improved durability and performance in radiation therapy equipment and medical imaging devices.

Keywords: Ti concentration; lattice parameters; ternary alloys Cu-Fe-Ti; X-ray diffraction; Miller indices, Radiation Therapy, medical imaging.

Introduction

Titanium is an important engineering material due to its useful combination of properties. These properties include corrosion resistance, retention of mechanical strength at high temperatures, and high specific mechanical properties resulting from titanium's low density and high strength [1]. These added elements, known as beta stabilizers, are categorized as isomorphous or eutectoid based on their phase behavior with titanium. Additionally, powder metallurgy offers benefits, including high material yield and reduced machining requirements, which are useful for decreasing the cost of titanium alloys compared to other structural metals [2].

Copper alloys are widely used in many applications due to their excellent properties, such as mechanical strength, electrical conductivity, thermal conductivity, and corrosion resistance. However, strengthening copper alloys through traditional methods like introducing defects inevitably decreases electrical conductivity due to increased electron scattering[3]. Synthesized nano-twinned copper, which had much higher strength but retained high conductivity, demonstrated this dilemma could be resolved through microstructure design. The nano-twinned alloys made by special methods like electrodeposition have limited sample sizes unsuitable for industrial use. Among strengthening approaches, precipitation strengthening effectively improves copper alloy strength without decreasing conductivity much [4]. Copper and iron are some of the most affordable and abundant eutectoid beta-stabilizer elements that can be utilized to produce alpha-beta titanium alloys. Regarding binary titanium-copper alloys, some studies have prepared Ti-x Cu (x = 5 and 10 wt%) [5] .alloys using high-purity titanium and copper powders that were ball milled followed by hot pressure sintering under vacuum to produce samples. The sintering parameters were typically 800-1050°C under argon or vacuum conditions [6]. After sintering, additional Processing, like extrusion, was sometimes applied. The produced samples were in the form of cylindrical bars or discs of varying dimensions. Other researchers have employed similar fabrication routes to produce titanium-copper alloys with copper contents ranging from 2-25 wt%. More novel methods like microwave sintering have also been evaluated for consolidating titanium and iron powders into binary alloys [7]. However, some initial work has produced ternary titanium-iron-copper alloys via arc melting methods using titanium sponge, iron wire, and copper powders under an argon atmosphere. Further studies are needed to explore the processing-microstructure-property relationships in these ternary alloy systems fully.

The ternary alloys investigated often contained high levels of alloying elements, over 25%, placing them in the beta-titanium alloy category. Specific compositions like Ti-3.5 Cu Fe-3.9 have been fabricated to analyze mechanical performance, electrochemical behavior, and biocompatibility. Other work has focused on the semisolid Processing of titanium-copper-iron alloys via theorizing of arc-melted ingots [8]. Overall, the research indicates these ternary systems can offer a combination of properties, but further studies are still needed to fully characterize the relationships between Processing, microstructure, and properties. Past research on titanium alloys has extensively studied binary titanium-copper and titanium-iron systems, leading to alpha-beta and beta alloys. However, only limited work has examined ternary titanium-copper-iron alloys. The existing research on these ternary alloys has focused on compositions for beta-titanium alloys. The only study of alpha-beta ternary titanium-iron-copper alloys analyzed a single composition of Ti-3.5 Cu Fe-3.9. This reveals an opportunity to explore further the potential of simultaneously adding copper and iron to titanium to reduce costs while maintaining the favorable strength and toughness balance of alpha-beta alloys [9]. The goal of this research work is to improve the mechanical properties of mild steel using Cu-Fe-Ti alloy coatings and address the gap in knowledge by designing new ternary Copper-Iron-Titanium alloys with small additions of titanium in copper and iron alloy, targeting primarily alpha-beta microstructures. This work critically reviews the mechanical requirements and suggests ways of improving the mentioned properties for structural and many applications.

Material and Method

Highly purified chemicals are taken for the preparation of samples by electrochemical deposition. Electrodeposition is preferred over rival methods due to its credibility and low cost [10]. In addition, this technique has good control over its parameters and retains the ability to coat uneven geometrical surfaces. It also improves the physical appearance, extends life, and enhances the material's properties. Flow chart for the preparation of Cu-Fe-Ti alloy as shown in Figure 1.

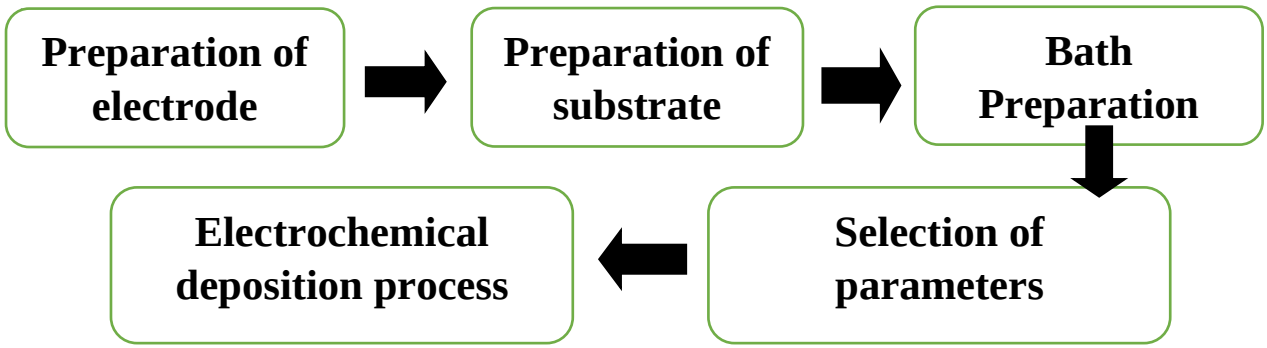

Fig. 1: Flow chart for the preparation of Cu-Fe-Ti alloy

Various parameters were employed for experimentation to achieve the expected results as show in the Table 1.

Table 1: Concentration of used chemicals with suitable operating parameters

Bath Parameters	Bath 1	Bath 2	Bath 3	Bath 4
$CuSO_4.7H_2O$ (M)	0.15	0.15	0.15	0.15
$FeSO_4.7H_2O$ (M)	0.15	0.15	0.15	0.15
$TiSO_4.7H_2O$ (M)	0	0.03	0.06	0.09
Boric Acid, H_3BO_3	0.25	0.25	0.25	0.25
Saccharine (g/I)	1.19	1.19	1.19	1.19
pH	4	4	4	4
Temperature (^{o}C)	27	27	27	27
Current density (A / m^2)	0.02	0.02	0.02	0.02
Deposition Time (min)	20	20	20	20

The experimental setup for electrochemical deposition was established. The substrate was attached to the fabricated electrode, then fixed with Tafton tape to secure the connection, and erected with a moving holder to hold the electrode. The electrodes were connected to the anode and the cathode. The power supply was used to supply current to the electrolytic bath via anode and cathode. The positive and negative ends of the main power supply were connected to the anode and cathode, respectively, with a distance of about 2 cm between the anode and the cathode.

Fig. 2: Apparatus setup for electrochemical deposition

The experiment was conducted in a 50mL Pyrex beaker before each use, the device was thoroughly washed with distilled water and cleansed with ethanol. Hot air drying was utilized after washing to ensure the beaker was clean before making the bath solution [11]. An electrochemical cell was constructed to perform experiments before bathing. The cell consisted of two electrodes area (1 x 1) cm^2 low-carbon steel cathode and a larger graphite anode rod. This setup was assembled and used prior to each bath to carry out the experimental procedure[12]. The anode was polished with emery paper, washed with distilled water and ethanol, and dried with hot air prior to each use. When an electric current was applied to the anode for 20 minutes, the anode partially dissolved into the electrolyte solutions. The dissolved metal ions in the electrolyte solution became reduced at the solution-cathode interface, resulting in metal coating deposition onto the cathode surface as shown in Figure 2.

Each layer was stripped after electrodeposition and dipped once in distilled water to prevent oxidation of the coating surface [13]. The substrate was weighed and dried using heated air. The thin film thickness was calculated by determining the weight difference of the substrate prior to and following the deposition process. The substrate was then adhered with double-sided tape and enclosed in a sealed box for further analysis. The formula for calculating the thickness formula is that

$$t = m/\rho A \qquad (1)$$

Here m is the mass of the alloy in grams, A represents the deposition area in centimeters, and the ρ average density of the deposit is. Therefore, the unit of thickness is centimeters. Characterization techniques involve X-ray diffraction for structure determination. A scanning electron microscope generates images of a sample's surface by scanning it with a focused electron beam [14]. The electrons interact with the sample's atoms, generating signals that provide information about the morphological and compositional properties of the surface. X-ray spectroscopy techniques can analyze the energy spectrum of the emitted X-rays to quantify the presence of specific elements in the sample.

Results and Discussion:

The thickness of electrodeposited Cu-Fe-Ti alloy was calculated according to the above Equation (1), and the results are presented in Table 2

Table 2: Concentration of Ti, deposited Mass, and thickness of Cu-Fe-Ti coated alloys.

Sample Name	Deposited mass (g)	Thickness (μm)
Cu-Fe-Ti (0.000 g)	0.05	62.87
Cu-Fe-Ti (0.354 g)	0.04	50.37
Cu-Fe-Ti (0.716 g)	0.03	37.81
Cu-Fe-Ti (1.074 g)	0.02	25.22

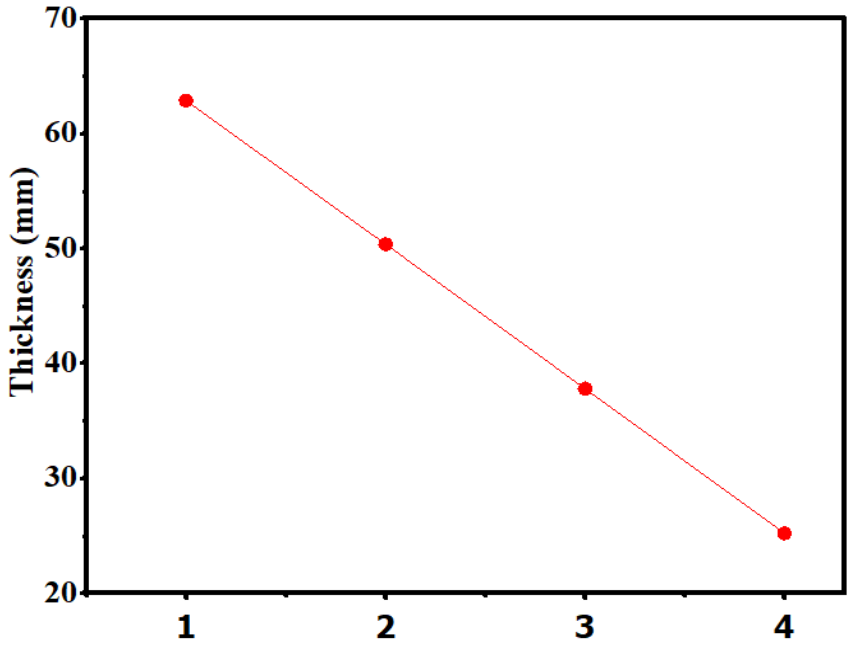

Fig. 3: Thickness of the Cu-Fe and Cu-Fe-Ti alloy coatings

A graph is plotted between the Ti concentration and thickness of the samples in Figure 3. The curve shows the decreasing thickness trend with increased Ti contents. Thickness mainly depends on the deposited Mass of the samples. The thickness decreases as the deposited Mass decreases with an increase of Ti. This decrease in deposited Mass can be attributed to the density of the samples. Since the density of Ti is less than the average density of the Cu-Fe alloy, increasing Ti contents decreases the density of the samples; hence, the coated alloys' thickness. One of the purposes of this work is to study the effects of adding Ti content on the structure and properties of binary Cu-Fe alloy. The results of these Cu-Fe-Ti alloys have been discussed in the sections below.

XRD data from ternary Cu-Fe-Ti alloy coatings were used to identify the phases in the prepared samples. All reflections are indexed according to the procedure described in B. D. Cullity's standard procedure. X-ray diffraction graphs are plotted between intensity (a.u) and 2θ (deg). The peaks are obtained at the Miller Index (111), (200), and (220), as shown in the X-ray diffraction pattern, respectively. These peak reflections give information about the composition and the phases present in the samples. The Miller indices show that the structure of the alloy is face-centered cubic with lattice parameters given in Table 3. The variation in the intensities of the patterns is given from 0-150 (a.u) and variation in the angle 5-100°. The peak (220) is more intense than the rest of the mixture's peaks.

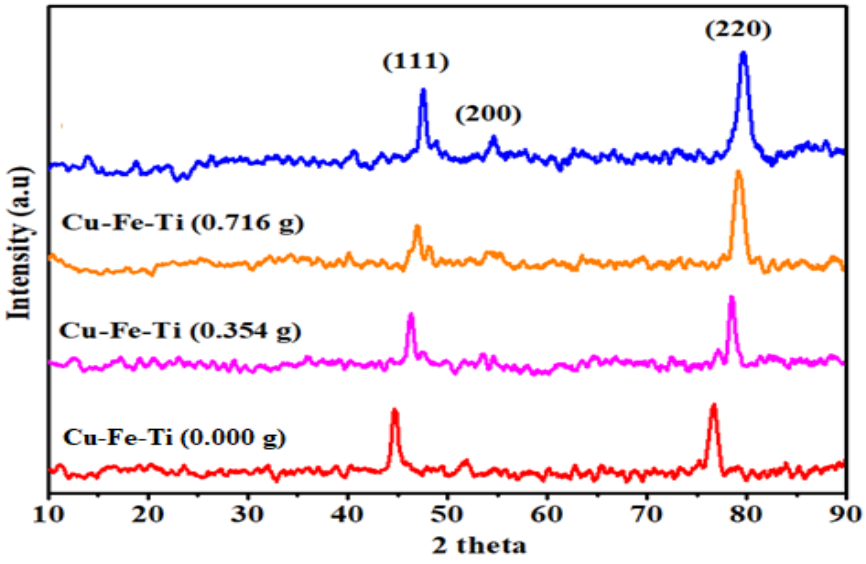

Fig. 4: Stacking of XRD patterns for all studied samples of alloys

The room temperature XRD pattern of the Cu-Fe alloy with sharp peaks at diffraction angles of 44.7°, 51.9°, and 76.7° as shown in Fig. 4. This figure shows the corresponding intensities 113, 36, and 121 of the given angles. Indexing the data using the standard method shows that the sample has a face-centered cubic (fcc) structure. The highest peak position with miller indices (111) and the other with miller indices (200) and (220) according to diffraction angles are determined.

In Fig. 4, all reflections show a face-centered cubic structure, and there is no indication of the superlattice peaks. So, there is an absence of superstructure in all the samples. The graph shows that as the concentration of Ti

increases gradually, then the intensity peak moves right. The addition of Ti also changes the unit cells' dimensions, as shown in Table 3. The lattice parameters of Cu-Fe-Ti alloy are calculated using the X-ray diffraction data, and the results are tabulated in Table 3. The X-ray wavelength used in these experiments was 1.54 Å. The peak position with miller indices (111) lies from 44.7° to 44.7° diffraction angle for all samples. The peak position with miller indices (220) lies from 76.7° to 76.7° diffraction angle for all samples.

Table 3: Miller indices and lattice parameters taken from X-ray diffraction measurements of Cu-Fe-Ti alloy

Sr No.	Sample Name	Hkl	Lattice parameter (Å)
1	Cu-Fe-Ti (0.000 g)	1 1 1	3.506
		200	
		2 2 0	
2	Cu-Fe-Ti (0.354 g)	1 1 1	3.501
		200	
		2 2 0	
3	Cu-Fe-Ti (0.716 g)	1 1 1	3.498
		200	
		2 2 0	
4	Cu-Fe-Ti (1.074 g)	1 1 1	3.497
		200	
		2 2 0	

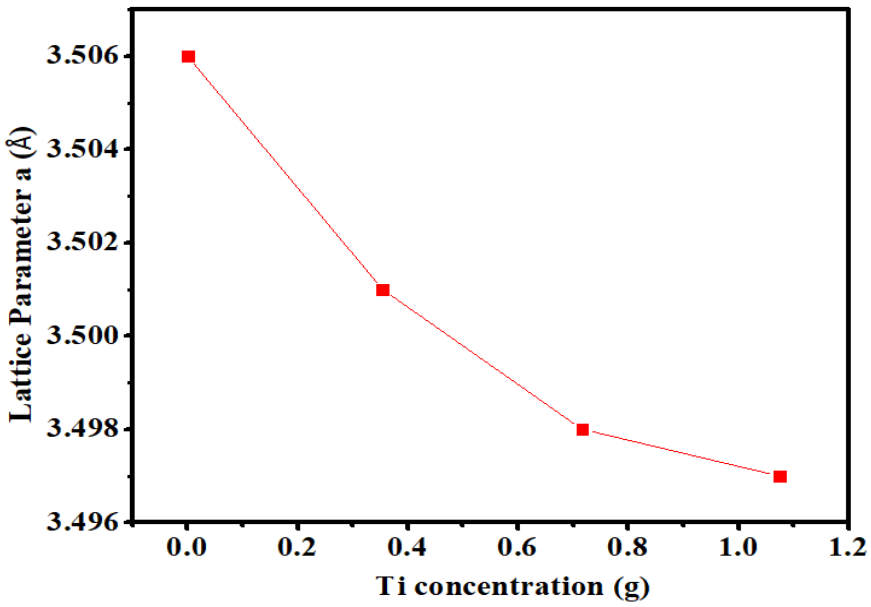

Fig. 5: Ti Concentration dependence of lattice parameter of Cu-Fe-Ti alloys

The data shows that as the concentration of titanium (Ti) increases as shown in Table 3 and Fig 5, the lattice parameter of the alloy decreases. This trend can be attributed to the smaller atomic radius of titanium compared to copper (Cu) and iron (Fe). The decrease in lattice parameter is more pronounced at lower Ti concentrations. At higher Ti concentrations, the rate of decrease slows down. This trend suggests that at low Ti concentrations, the substitution of the larger Cu and Fe atoms by the smaller Ti atoms causes a more significant reduction in lattice parameter. However, as more Ti is added, there are fewer sites left for substitution by Ti, so the effect on lattice parameter is diminished. Overall, the decreasing lattice parameter reflects the incorporation of the smaller Ti atom into the Cu-Fe alloy lattice. So, when the Ti concentration is increased, the lattice parameters of the coated alloy sample decrease. This decrease in lattice parameter is also probably due to the preference of Ti concentration. That's why the lattice parameters of the Cu-Fe-Ti alloy decrease. The surface morphology of the plan view of the coatings is observed through a scanning electron Microscope (S.E.M.), as shown in Fig 6 (a-d).

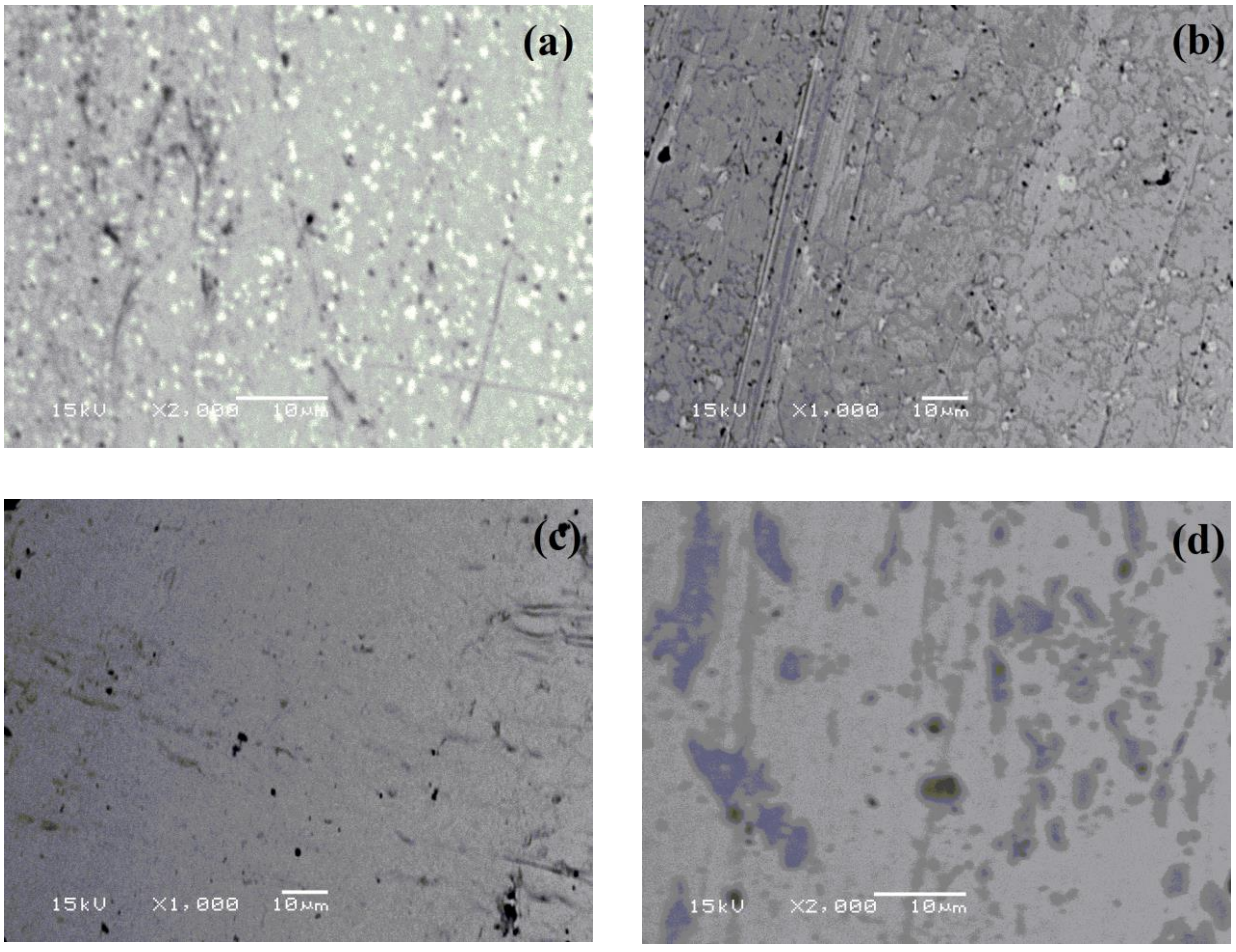

Fig. 6 (a) SEM image of Cu-Fe-Ti, (b) SEM image of Cu-Fe-Ti (0.354g), (c) SEM image of Cu-Fe-Ti (0.716g), (d) SEM image of Cu-Fe-Ti (1.074g)

All these images were taken out for Cu-Fe-Ti alloys at different Ti concentrations. Micrographs show that the coating has granular morphology for that sample, which has zero concentration of Ti. But as the Ti concentration is increased, the grains start to disappear. As the concentration of Ti increases, the size and numbers of the grains decrease. Further addition of Ti results disappears of grains, and the new phases have appeared in the last sample. Surface smoothness is also improved by increasing Ti concentration, as shown in micrographs. Such material could be associated with attractive mechanical properties and less mass deposition due to the formation of Cu-Fe inter-metallic preceding the nucleation of Ti coating on the substrate going to uniform form.

In conclusion, the composition and phase structure influence the surface morphologies of the coating as the surface smoothness of samples increases with increasing Ti content so that it can be related to the thickness of the samples. The samples showed a trend of decreasing thickness as the percentage of titanium increased. Scanning electron microscopy of sample 4, which had the highest titanium content, revealed a smooth surface morphology without detectable defects such as pores or segregation after the electrodeposition process. This suggests that increasing the titanium percentage results in smoother and more uniform coatings.

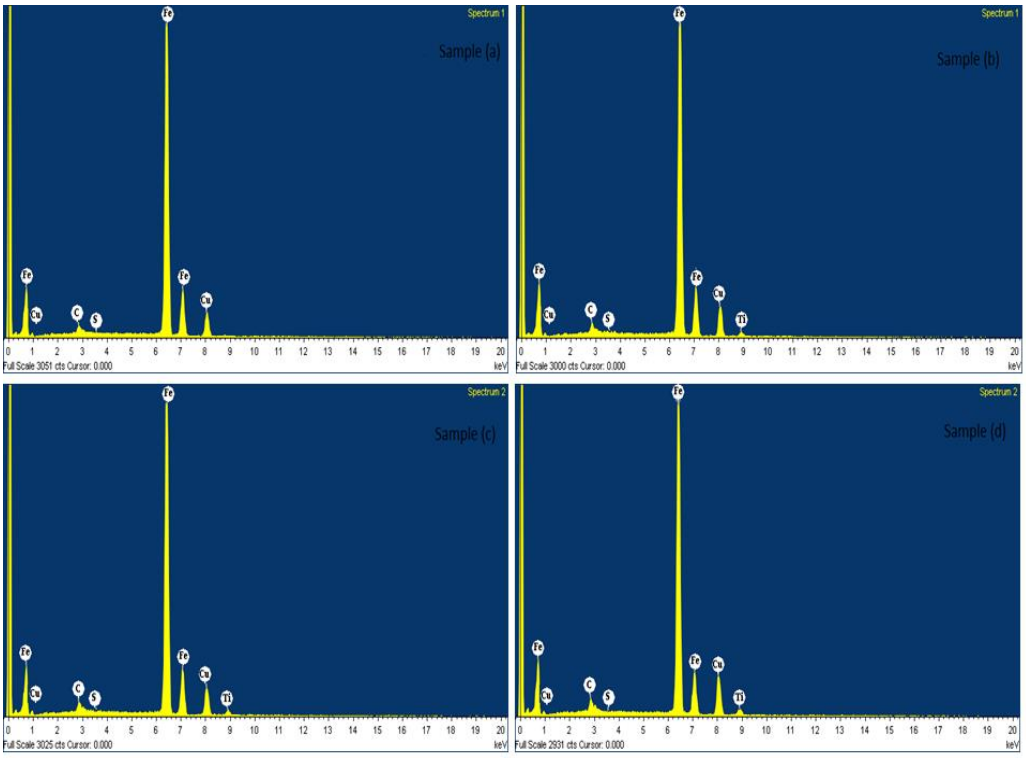

Fig 7 (a-d) EDX peaks of the mild steel substrates and coatings showing elemental concentrations.

From sample (a) is shown in **Figure 7**, it can be seen clearly that two peaks are observed in the samples. The high peaks of Fe show that Fe_3C, which confirms the mild steel substrate and the low peak of Fe in E.D.X. data represent the β-Fe phase present in the sample. There is no Ti peak in the sample, which confirms that the sample (a) is prepared without Ti.

Other samples showed E.D.X. analysis of the mild steel substrate used for the Ti concentration. The energy dispersive data showed the main peaks of Fe, Ti, Cu, carbon, and sulfur. From samples (a-d), it can be observed that except sample (a), all other samples have Ti peaks, confirming Ti's presence in the samples. It can also be observed that the increase in the Ti sample gradually confirms the increase in Ti contents. The Ti, Cu, and Fe presence in samples after alloying confirmed the Effect of the deposition of all three elements. Mechanical properties are an important factor in measuring product quality and hardness, and tensile tests are commonly used to investigate the mechanical properties of the coating. A material and its ability to withstand loads without fail is a measure of its flexibility.

Many methods are used to measure the hardness of materials. Vicker's hardness is also microhardness, especially used to measure the hardness of metals and alloys accurately. This method is used for sophisticated materials. The hardness of each sample and the substrate's hardness is measured at room temperature, and the obtained data is shown in Table 4. This data of hardness is taken at different concentrations of Ti. The data shows that coating of alloys on a substrate increases the samples' hardness.

Table 4: Vicker's Hardness (H.V.H.V.) of Cu-Fe-Ti alloys using Vicker's hardness tester

Sample Type	Vickers Hardness (HV)
Substrate	254.900
Cu-Fe-Ti (0.000 g)	316.544
Cu-Fe-Ti (0.354 g)	373.851
Cu-Fe-Ti (0.716 g)	414.120
Cu-Fe-Ti (1.074 g)	443.993

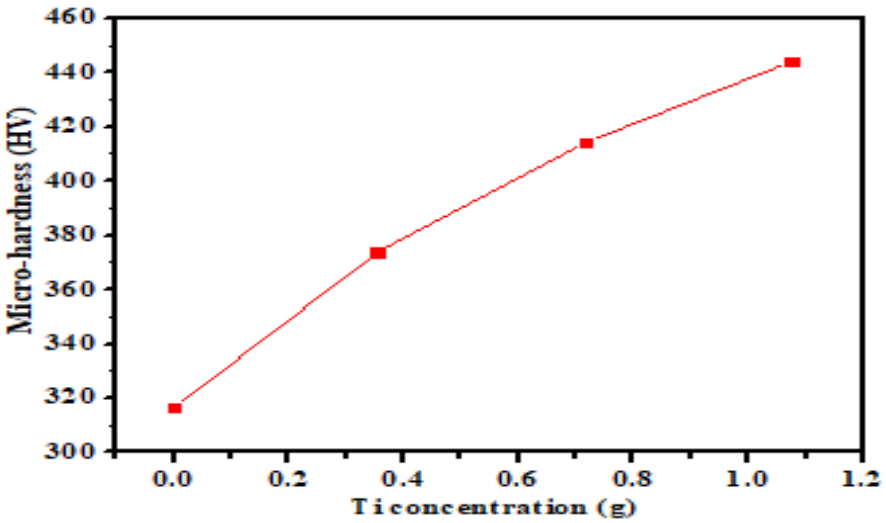

Fig. 9: Micro-hardness (H.V.H.V.) of Cu-Fe-Ti alloys at various Ti contents

A graph plotted between micro-hardness and Ti concentration is shown in Fig. 9. The curve in the figure shows the increasing trend of hardness. The curve also shows that at a low concentration of Ti, the increasing trend is faster from 316 HV to 375 HV, but at a higher concentration of Ti, the increase becomes slow. The hardness of Ti is much higher than that of Cu and Fe. So, When the Ti concentration is increased, the hardness of the coating and the sample are increased. This increase in hardness is also probably due to the preference of Ti concentration. That's why the hardness of the Cu-Fe-Ti alloy increases.

The increase in micro-hardness can also be attributed to the change in microstructure, as shown in Fig. 9. At low concentrations of Ti, the voids are present in the samples, but as the Ti concentration is increased, the voids are decreased. The voids completely disappear even for the last sample where the Ti contents are maximum. Mechanical properties can also be related to the lattice parameters of the samples. Fig. 5 shows the decreasing trend of lattice parameter with increasing Ti concentration. As the lattice constant decreases, the lattice volume also decreases, and the coating becomes more compact, increasing hardness. The increase in the hardness of the coating can be attributed to the Ti hardness of the samples. Since Ti has a higher value of hardness than the hardness of Cu and Fe increasing Ti concentration in the coatings increases their hardness as shown in the Table 4.

Conclusion

The electrodeposition of ternary Cu-Fe-Ti alloys on mild steel substrates was investigated. X-ray diffraction analysis revealed the deposited alloys exhibited a single-phase, face-centered cubic crystal structure across all samples. The lattice parameters were found to be highly dependent on the relative compositions of Cu and Fe. Scanning electron microscopy imaging showed the coatings became smoother with increasing Ti content. Additionally, the mild steel substrates coated with Cu-Fe-Ti alloys displayed a decreasing trend in film thickness as the titanium concentration in the deposition solution was increased. The smoother morphology of the coatings with higher titanium suggests improved mechanical properties of the mild steel substrates. Overall, the study demonstrates that varying the composition of electrodeposited Cu-Fe-Ti alloys can tailor the crystal structure, morphology, and potential mechanical properties of the resulting coatings on mild steel. Cu-Fe-Ti alloy coatings significantly enhance mild steel's mechanical properties, making it a promising candidate for applications in radiation environments, such as nuclear power plants and medical equipment. This research contributes to the development of radiation-resistant materials.

Acknowledgement: We would like to express our sincere gratitude to Dr. Kafiz of Gomal University D.I Khan for his invaluable guidance and support. Additionally, we are grateful for providing us Labs, which was essential to the progress of this research. We would also like to extend our special thanks to our group mate Muhammad Rehan for generously sharing his expertise and time. His specialization is in material science field, which significantly contributed to the completion of multiple research papers.

References

1. Totten, G. and D.J.A.H.D.J.A.H. MacKenzie, Introduction to Titanium and its Alloys. 2016. 4.
2. Kang, L. and C.J.A.E.M.C.J.A.E.M. Yang, A review on high-strength titanium alloys: microstructure, strengthening, and properties. 2019. 21(8): p. 1801359.
3. Tyler, D.E. and W.T. Black, Introduction to copper and copper alloys. 1990.
4. Lin, H., et al., Stress relaxation behaviors and mechanical properties of precipitation strengthening copper alloys. 2021. 861: p. 158537.
5. Paul, M., Fabrication and characterization of novel low-cost ternary titanium alloys. 2021, The University of Waikato.
6. Akbarpour, M.R., et al., Processing and microstructure of Ti-Cu binary alloys: a comprehensive review. 2022. 127: p. 100933.
7. Newby, E.B., Investigation of in-situ alloying grade 23 Titanium with Copper by Selective Laser Melting Process for biomedical applications. 2018.
8. Bosman, H.L., Influence of powder particle size distribution on press-and-sinter titanium and Ti-6Al-4V preforms. 2016, Stellenbosch: Stellenbosch University.
9. Zadorozhnyy, V.Y., et al., Electrochemical behavior and biocompatibility of Ti-Fe-Cu alloy with high strength and ductility. 2017. 707: p. 291-297.
10. Gerdemann, S.J.J.A.m. and processes, Titanium process technologies. 2001. 159(7): p. 41.
11. Wu, B. and A.J.A.P.R.A.J.A.P.R. Kumar, Extreme ultraviolet lithography and three-dimensional integrated circuit—A review. 2014. 1(1).
12. Hassid, W. and S. Abraham, [7] Chemical procedures for analysis of polysaccharides. 1957.
13. Masoudi, M., M. Rahimnejad, M.J.I.J.o.H.E. Mashkour, Enhancing operating capacity of microbial fuel cells by using low-cost electrodes and multi anode-cathode connections in a membrane-less configuration. 2021. 46(11): p. 8226-8238.
14. Moreira, T.A.S., Nanostructured Polythiophene Materials for Electrochromic Applications. 2022.